Charge fluctuations in capacitive DNA sequencing with graphene nanopores

Gustavo T. Feliciano,[1,2] Carlos Sanz-Navarro,[3] Mauricio Domingues Coutinho-Neto,[2] Pablo Ordejón,[3] Ralph H. Scheicher,[4] and Alexandre Reily Rocha[1]

[1] *Instituto de Física Teorica, Universidade Estadual Paulista (UNESP), São Paulo, SP, Brazil*
[2] *Centro de Ciências Naturais e Humanas,Universidade Federal do ABC, Santo André, São Paulo, Brazil**
[3] *Institut Catalá de Nanotecnologia - ICN2- Universidad Autonoma de Barcelona, Barcelona, Spain*
[4] *Division of Materials Theory, Department of Physics and Astronomy, Uppsala University, Uppsala, Sweden*

(Dated: December 13, 2013)

The advent of parallelized automated methods for rapid whole-genome analysis has led to an exponential drop in costs, thus greatly accelerating biomedical research and discovery. Third-generation sequencing techniques, which would utilize the characteristic electrical conductance of the four different nucleotides, could facilitate longer base read lengths and an even lower price per genome. In this work, we propose and apply a quantum-classical hybrid methodology to quantitatively determine the influence of the solvent on the dynamics of DNA and the resulting electron transport properties of a prototypic sequencing device utilizing a graphene nanopore through which the nucleic acid chain is threaded. Our results show that charge fluctuations in the nucleotides are responsible for characteristic conductance modulations in this system, leading to a field effect transistor stabilized by the dynamic aqueous environment.

INTRODUCTION

Nucleotides form the building blocks of DNA. The information encoded by their ordered arrangement in the nucleic acid chain provides the set of instructions for all processes occuring in any living being on this planet. Thus, determination of the whole genome sequence is the key to a fundamental understanding of a wide range of biologically relevant issues, ranging from evolutionary developments to finding genetic predispositions for hereditary pathologies.[1] Although we have witnessed a dramatic decrease in the cost of genome sequencing over the past five years [2], this price development has recently shown signs of asymptotic convergence (to a value of slightly below USD 10,000 per genome), mainly due to the expenses of chemical reagents required in the process. Thus, whole-genome sequencing still remains too costly for widespread routine application in healthcare, delaying the onset of personalized or precision medicine.[3]

An alternative approach for DNA sequencing, that holds the potential to be several orders of magnitude less expensive, is the possibility of using nano-sized pores in biological [4–8] or solid-state [9–14] membranes as a sieve for DNA strands to pass through. During this translocation process one aims at identifying the different nucleotides momentaneously residing within the pore. If the four base types (adenine, guanine, cytosine, and thymine) could be differentiated through a physical mechanism then this approach would allow for rapid whole-genome sequencing without the usual requirements of DNA amplification or labeling. The discrimation could be accomplished through a variety of techniques, for example, by measuring the subtle changes in ionic current through the pore due to characteristic blockage by the different bases [7, 8, 15, 16]. Alternatively, it has been theoretically proposed [17] and later experimentally demonstrated [18–20] that one could differentiate between each nucleobase by measuring the transverse tunneling current across DNA in the pore. The fundamental idea here centers on the fact that each nucleotide has a different electronic structure and, more importantly, couples differently to the electrodes [21], which characteristically affects the electronic transport properties. Different signatures in the conductance of each base could thus provide the means for sequencing DNA [21, 22].

Within the solid-state nanopore family, one material has recently gained considerable attention: graphene [23], an atomically thin membrane, which possesses a number of intriguing electrical and mechanical properties [24, 25], in partcular high conductivity. The almost negligible thickness of graphene holds the best chances for the desired single-base resolution in electrical DNA sequencing, as in a nanofabricated gap based on the current flowing between the sharp edges of two semi-infinite sheets of graphene acting as transverse electrodes [26]. Experimentally, it was shown shortly after this proposal that it is indeed possible to drive DNA through a nanopore in graphene and detect its presence via changes in ionic current [27–29]. Very recently, it was experimentally achieved to detect the translocation of DNA through a nanopore in a graphene nanoribbon simultaneoulsy by drops in the ionic current and peaks in the transverse electric current [30].

There have been a number of theoretical investigations on nanopores in graphene for the application of DNA sequencing. [31–36] Most of these studies have focused on the use of a graphene nanoribbon (GNR),[34, 35] where the edge states play a major role in the transport. Most importantly, a proper theoretical description has to take into consideration both dynamical and environmental effects [37] from the water molecules and the counter-ions.

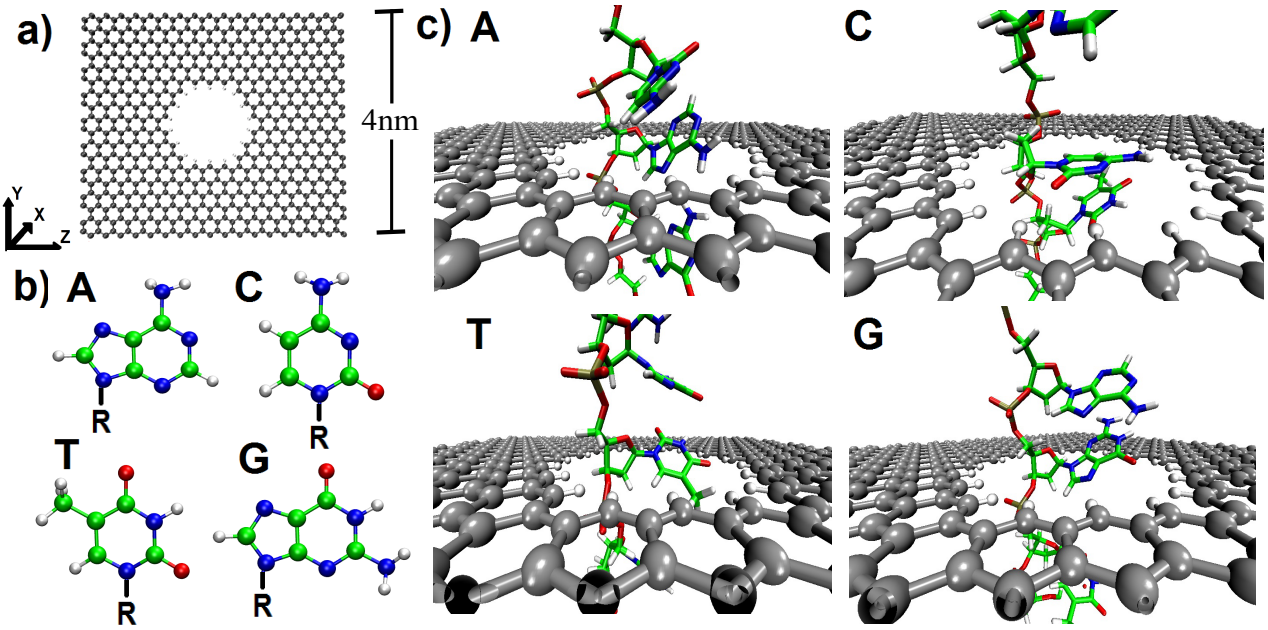

FIG. 1: a) Schematic representation of the 1.3 nm wide graphene nanopore model used in our simulations. The transport occurs along the z-direction. b) The four nucleobases, A, C, T, and G, occurring in DNA. Carbon atoms are shown in green, nitrogen in blue, oxygen in red, and hydrogen in white. R indicates the not-shown sugar-phosphate part that completes the nucleotide. c) Typical snapshots from the molecular dynamics simulations for each of the four nucleobase types located within the graphene nanopore. For clarity, water molecules and counterions have been removed from the image.

Although a few of these issues have been addressed in the past, mostly either model Hamiltonians [32, 35, 37] or very specific configurations [22, 34] were used.

A number of important questions are thus left open. In particular, it remains unclear whether it is possible to differentiate between the four different nucleotides in the simplest possible graphene nanopore configuration using transverse conductance measurements. In order to answer these questions, we present here a systematic study of the electronic transport properties of a single-stranded DNA molecule within a graphene nanopore. A combination of density functional theory coupled to hybrid classical methods is utilized by us to take into consideration the effects of the solvent [38, 39] together with a Green's function formalism to calculate the electronic transport.

METHODOLOGY

The system studied by us comprises a square-shaped graphene sheet of dimensions 4 nm × 4 nm containing a nanopore. This was created by selectively removing carbon atoms to form a hexagonal-shaped orifice, approximatenly 1.3 nm wide, enclosed by zigzag edges (Figure 1a). The size of the nanopore was chosen as a compromise between experimental fabrication feasibility [27, 28] and consideration for the computational expenses of the simulations. Dangling bonds, created by the removal of carbon atoms, were saturated with hydrogen atoms. This graphene nanopore was completely immersed in water with counter ions present. We simulated both the empty pore as well as the case when a four-base single-stranded DNA (ssDNA) molecule is present, containing the four nucleotides occuring in DNA (Figure 1b). Each nucleotide possesses one negative charge localized in its phosphate group.

For our simulations, first, we sample the possible configurations of the DNA molecule and the solvent for each nucleobase type residing in the graphene nanopore using classical molecular dynamics (MD) simulations. The system comprises a 35 Å × 40 Å ×40 Å box containing 4400 water molecules and 0.2 M Na and Cl counterion concentration. An imbalance of 4 extra Na^+ ions was introduced to compensate the 4 negative charges from the phosphate groups of the ssDNA molecule, thus keeping the entire system neutral. The standard all-atom version of the AMBER99SB [40] empirical force field was used in the GROMACs [41] package to describe the interatomic potentials. We used the SPC water model [42] and parameters for benzene to model graphene, with partial charges only in the hydrogen atoms terminating the nanopore edges and their neighboring carbon atoms.

We decided not to simulate here any actual translocation processes of DNA through the pore, since the achievable simulation time is far from sufficient to approach any reasonable speed of DNA in experiment. Rather, our aim was to sample over the fluctuations of a given nucleotide in the pore during the simulation time to max-

imize the statistical data obtained. As an initial configuration, each base was placed in the pore and a thermalization procedure was performed for 100 ps at 300K using an NVT ensemble. We then equilibrited the water density for a further 200 ps using an NPT ensemble at 300K and 1 bar with a Nose-Hoover thermostat and Parrinello-Rahman barostat. In both cases, we restricted the movement of the nucleotide by preventing it from moving outside the pore, but allowing free movement in the plane of the graphene sheet. Finally, in the production stage, a 300 K NVT 2000 ps MD simulation is performed where all the atoms are free to move. From the resulting trajectories, 90 snapshots are randomly extracted from each passing nucleotide, spaced in time by 20 ps (*i.e.*, 20,000 1-fs time-steps). Typical snapshots obtained in our simulation are shown in Figure 1c, and all the sampled configurations are shown in Figure S1 (supporting information).

To determine the electronic structure of the system under the external perturbation of the environment, the whole system is partitioned into a quantum mechanical (QM) system, comprised by the graphene sheet containing the nanopore and the passing nucleotide (between 646–648 atoms, depending on the nucleobase) and a molecular mechanics (MM) system which includes all the water molecules, the counter ions, and the nucloetides which are not, at a given instance, inside the pore. The QM system is treated by first-principles calculations based on density-functional theory (DFT) [43, 44], using the gereneralized gradient approximation (GGA) for the exchange and correlation potential in its PBE form [45]. Core electrons were replaced by norm-conserving pseudopotentials. The Kohn-Sham wave-functions for the valence electrons were expanded in a double-ζ polarized (DZP) basis sets for the nucleotide atoms and a double-ζ (DZ) basis set for the graphene membrane. The calculations were carried out using the SIESTA code,[46] with Brillouin zone sampling only carried out at the Γ-point due to the size of the system. The MM potential is included as an external potential acting on the Kohn-Sham Hamiltonian.

Finally, once the Hamiltonian for each snapshot is obtained, we calculate the zero-bias transmission coefficients using the equilibrium Green's function formalism [47] as implemented in the SMEAGOL package [48, 49]. A strip of 108 atoms from the left and right sides of the graphene nanopore are taken as the electrodes.

RESULTS AND DISCUSSION

Figure 2a illustrates how much the conductance of the graphene nanopore is changing when the dynamical environment of water and counter ions are introduced in the system (but no DNA molecule yet). Specifically, we have plotted here the averaged difference in conductance

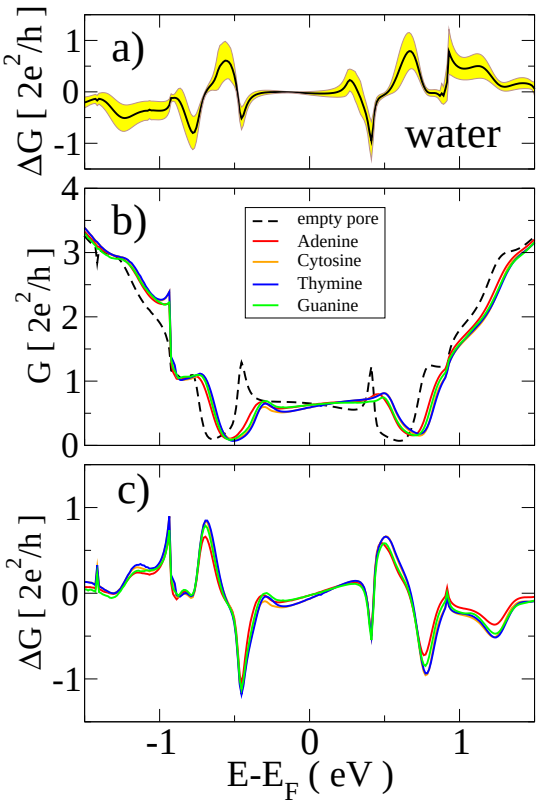

FIG. 2: a) The black curve shows the averaged difference in conductance as a function of energy between the empty (dry) pore and the molecular dynamics simulation of the pore containing water and counter-ions. The yellow area enveloping the black curve corresponds to ± one standard deviation from the mean. b) Colored curves show the average conductance as a function of energy for each of the four DNA nucleotides when located in the pore with water and counter-ions present. The black dashed line shows the conductance of the empty (dry) pore as a reference. c) Averaged difference in conductance between the empty (dry) pore and the molecular dynamics simulations of the four different nucleotides including the solvent and counter-ions.

between the pore with water molecules and counter ions present and the empty (dry) pore. We note that, while there are changes to the conductance for a wide range of energies, specifically at the Fermi level, the average change and the standard deviation tend both to zero. In Figure 2b, we show the averaged total conductance of the pore with the four different nucleotides present (including solvent effects), comparing it to the conductance of the empty (dry) pore as a reference. One notices that the curves for each of the DNA nucleobases are very similar. This becomes further observable in Figure 2c where the averaged difference in conductance relative to the empty (dry) pore is plotted for the four different nucleotides present.

It can be clearly seen that the presence of DNA affects conductance strongly. Overall, a shift can be ob-

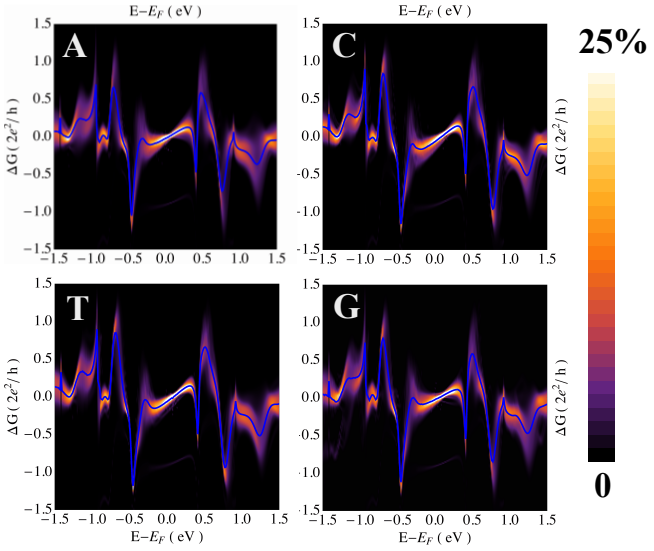

FIG. 3: Here the conductance distributions for the four different nucleotides in the graphene nanopore are plotted as a function of energy. Blue curves show the average conductance (as already plotted together in Figure 2c) while the enveloping shaded areas (with the color gradient ranging from black over violet, orange, yellow to white) indicates the percentage with which deviations from the average occur in the conductance at different energies for the four nucleotides.

served, with prominent features of the conductance curve for the empty pore being shifted towards higher energies when DNA is present. This shift is also observed when only solvent molecules are present, albeit to a smaller degree. Furthermore, relatively sharp features present in the curve for the empty pore, such as peaks near $\pm$ 0.5 eV and $\pm$ 1 eV, are suppressed when DNA is introduced to the pore. These resonances can be associated with localized states similar to those expected to be present on the edges of graphene nanoribbons [50]. The more drastic changes can be seen most clearly in Figure 2c. Here, the suppression of peaks can be recognized as sharp peaks, while smoother shapes result for the shifts in areas where the conductance is relatively slowly changing as a function of energy. This shift is mostly due to the fact that the nucleotides tend to become negatively charged. It thus creates an electric field which acts as a local gate on the graphene nanopore.

The difference in averaged conductance between the four DNA nucleotides is seen, from both panels b and c in Figure 2, to be rather similar for most energies, thus not allowing one to easily distinguish between the four nucleotides based on average value of conductance alone. However, as we will discuss below, the actual statistical distribution of conductance values does show some characteristic differences, in particular between the group of purine nucleobases guanine and adenine on the one hand, and the pyrimidine nucleobases cytosine and thymine on the other hand. Figure 3a shows the distribution of values of conductance change as a function of energy for each one of the basis. As before, albeit some differences can be observed, they are all qualitatively similar. When one focuses on the Fermi level, however, the differences become more noticeable.

In Figure 4, therefore, we plot the conductance histogram for each of the four nucleotides at the Fermi energy E_F. Albeit small, there are clearly apparent differences discernible between the two families of nucleobases, namely the purines (A and G) and pyrimidines (C and T). Although similar, the ratio between the peaks of the distributions of adenine and thymine, for example, is approximately 1.5, whereas for adenine and guanine, and thymine and cytosine, the difference is approximately 5% and 12%, respectively. However, the dynamical effects lead to a large broadnening of the distributions and they all tend to significantly overlap.

At the same time, we can highlight a different sensing mechanism for detecting the DNA nucleotides. While in most works tunnelling has been considered, graphene is higlhy conducting. As our calculations show, the nucleotides tend to be negatively charged. The charged nucleotides create an electric field that changes the local chemical potential around the pore in way similar to a field effect transistor. As we allow the molecule to move freely inside the pore, there are small charge fluctuations due to the interaction with the graphene sheet, which in turn influence the conduction. This is evidenced by the histogram of the net charge on each of the nucleotides, which is presented in figure 4b. We can clearly see a one-to-one correspondence between the two distribustions. Finally we notice that the purines comprise two aromatic rings. The larger size implies that the interation with the graphene sheet. Water here plays an important role, not only in the dynamics of the system, but also for stabilizing the net charge on each nucleobase, as one observes in a number of biological systems [**?**]

CONCLUSIONS

In the present work, we investigated the possibility of using graphene nanopores as an all-electrical sequencing device for DNA, taking into account the structural fluctuations of the nucleobases and the noise of the solvent/counterions/DNA electrostatic potential within an electronic transport QM/MM approach. The developed method considerably reduces the computational effort and at the same time, captures the essential effects of the environment. The results show that the conductance difference between the nucleotides are considerably affected by the dynanics of the nucleobases within the pore. We also note that water is of fundamental importance in stabilizing the charged system.

We show that the fluctuations of the charge in each base lead to the same distribution in the conductance of

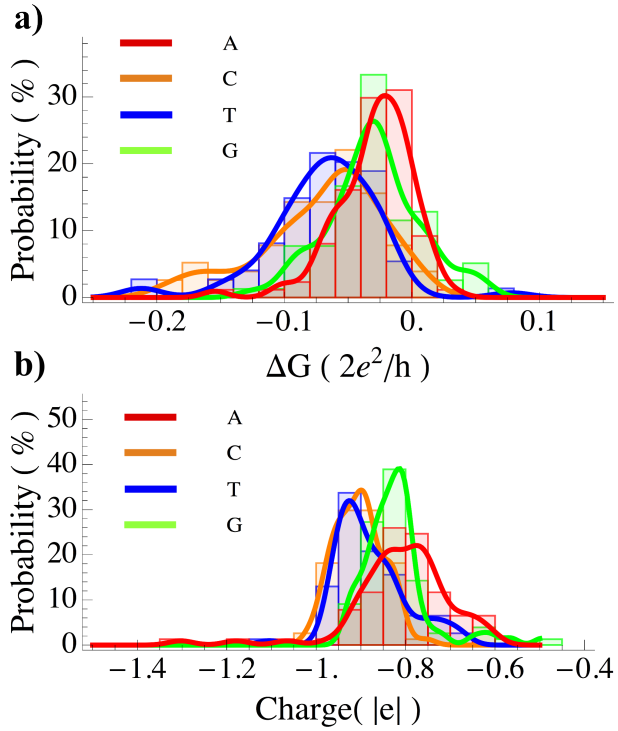

FIG. 4: a) Distribution of the difference in conductance at the Fermi level from the empty (dry) pore case for the four different nucleotides in the graphene nanopore, presented as histogram bars and fitted distribution curves. This plot is thus a combined cross-section of the data in Figure 3 at $E = E_F$. b) Charge distribution in the nucleotides presented as histogram bars and fitted distribution curves

each nucleotide. In essence, the charging of the base leads to an effective electric field in the graphene sheet which influences the conductance. This is an effect that cannot be captured by model Hamiltonians, which are not self-consistently calculated for each configuration. This capacitive transport mechanism can help explain experimental results for pores which are significantly larger than a single base, and would thus be extremely difficult to assess electronically through tunneling conductance.

Our findings leads us to conclude that all four nucleobase types will show similar conductances and that it would be hard to electrically distinguish between them in a graphene nanopore setup. Nonetheless, some degree of differentiation between the nucleobases appears to be possible. It is also important to note that the conducting pathways around the graphene nanopore yield larger transmission coefficients compared to those based on a tunneling current alone (e.g., in a nanogap). This could help to overcome the problem of noise in such devices. Finally, given the results of this work, functionalization of the atoms in the pore edge could significantly enhance nucleobase-pore interaction, the could on one hand reduce the structural noise by enhancing the graphene/nucleobase electronic coupling. At the same time they could be tailored for base-specific charge transfer. Hydroxide and amine groups are good candidates for functionalization. Hydroxide is expected to interact strongly with the nucleobases, due to the variety of possible interactions (it has a positive and a negative center of charge, plus the possibility fo hydrogen bonding). Nitrogen in the amine form would also be a good candidate, with two centers of negative charge and one center of positive charge, and they both resemble the groups already present in complementary nucleotides in double-stranded DNA. In view of these results, it seems that, although the sources of noise remain, functionalized graphene might still be engineered to yield better strategies for the development of electric DNA sequencing devices.

The authors would like to thank S. Sanvito for valuable discussions. We also acknowledge financial support from the São Paulo Research Foundation (FAPESP-Brazil - grant # 13/02112-0), CAPES-Brazil, UFABC, CNPq, the Swedish Foundation for International Cooperation in Research and Higher Education (STINT), and the Swedish Research Council (VR grant # 621-2009-3628).

* Current address: Instituto de Química, Departamento de Físico Química, Universidade Estadual Paulista (UNESP), Araraquara, Brazil

[1] F. S. Collins, E. D. Green, A. E. Guttmacher, and M. S. Guyer, Nature **422**, 835 (2003), ISSN 0028-0836, URL http://www.ncbi.nlm.nih.gov/pubmed/12695777.

[2] E. R. Mardis, Nature **470**, 198 (2011), ISSN 0028-0836, URL http://dx.doi.org/10.1038/nature09796.

[3] B. S. Shastry, The Pharmacogenomics Journal **6**, 16 (2006), ISSN 1470-269X, URL http://www.ncbi.nlm.nih.gov/pubmed/16302022.

[4] J. J. Kasianowicz, E. Brandin, D. Branton, and D. W. Deamer, Proceedings of the National Academy of Sciences of the United States of America **93**, 13770 (1996), ISSN 0027-8424, URL http://www.pubmedcentral.nih.gov/articlerender.fcgi?artid=19421\&tool=pmcentrez\&rendertype=abstract.

[5] D. W. Deamer and M. Akeson, Trends in Biotechnology **18**, 147 (2000), ISSN 0167-7799, URL http://www.ncbi.nlm.nih.gov/pubmed/10740260.

[6] G. M. Cherf, K. R. Lieberman, H. Rashid, C. E. Lam, K. Karplus, and M. Akeson, Nature Biotechnology **30**, 344 (2012), ISSN 1546-1696, URL http://www.pubmedcentral.nih.gov/articlerender.fcgi?artid=3408072\&tool=pmcentrez\&rendertype=abstract.

[7] E. A. Manrao, I. M. Derrington, A. H. Laszlo, K. W. Langford, M. K. Hopper, N. Gillgren, M. Pavlenok, M. Niederweis, and J. H. Gundlach, Nature Biotechnology **30**, 349 (2012), ISSN 1546-1696, URL http://www.ncbi.nlm.nih.gov/pubmed/22446694.

[8] G. F. Schneider and C. Dekker, Nature Biotechnology **30**, 326 (2012), ISSN 1087-0156, URL http://www.nature.com/doifinder/10.1038/nbt.2181.

[9] J. Li, D. Stein, C. McMullan, D. Branton, M. J. Aziz, and J. A. Golovchenko, Nature **412**, 166 (2001),

ISSN 0028-0836, URL http://www.ncbi.nlm.nih.gov/pubmed/11449268.

[10] A. J. Storm, J. H. Chen, X. S. Ling, H. W. Zandbergen, and C. Dekker, Nature Materials **2**, 537 (2003), ISSN 1476-1122, URL http://www.ncbi.nlm.nih.gov/pubmed/12858166.

[11] D. Fologea, M. Gershow, B. Ledden, D. S. McNabb, J. A. Golovchenko, and J. Li, Nano Letters **5**, 1905 (2005), ISSN 1530-6984, URL http://www.pubmedcentral.nih.gov/articlerender.fcgi?artid=2543124\&tool=pmcentrez\&rendertype=abstract.

[12] C. Dekker, Nature Nanotechnology **2**, 209 (2007), ISSN 1530-6992, URL http://www.nature.com/nnano/journal/v2/n4/full/nnano.2007.27.html.

[13] B. M. Venkatesan, D. Estrada, S. Banerjee, X. Jin, V. E. Dorgan, M.-H. Bae, N. R. Aluru, E. Pop, and R. Bashir, ACS Nano (2011), ISSN 1936-086X, URL http://www.ncbi.nlm.nih.gov/pubmed/22165962.

[14] A. Fanget, F. Traversi, S. Khlybov, P. Granjon, A. Magrez, L. Forró, and A. Radenovic, Nano letters (2013), ISSN 1530-6992, URL http://www.ncbi.nlm.nih.gov/pubmed/24308689.

[15] C. Sathe, X. Zou, J.-P. Leburton, and K. Schulten, ACS Nano **5**, 8842 (2011), ISSN 1936-086X, URL http://www.pubmedcentral.nih.gov/articlerender.fcgi?artid=3222720\&tool=pmcentrez\&rendertype=abstract.

[16] P. Xie, Q. Xiong, Y. Fang, Q. Qing, and C. M. Lieber, Nature Nanotechnology **7**, 119125 (2011).

[17] M. Zwolak and M. Di Ventra, Nano Letters **5**, 421 (2005), URL http://pubs.acs.org/doi/abs/10.1021/nl048289w.

[18] M. Tsutsui, M. Taniguchi, K. Yokota, and T. Kawai, Nature Nanotechnology **5**, 286 (2010), ISSN 1748-3395, URL http://www.ncbi.nlm.nih.gov/pubmed/20305643.

[19] S. Chang, S. Huang, J. He, F. Liang, P. Zhang, S. Li, X. Chen, O. Sankey, and S. Lindsay, Nano Letters **10**, 1070 (2010), ISSN 1530-6992, URL http://www.pubmedcentral.nih.gov/articlerender.fcgi?artid=2836180\&tool=pmcentrez\&rendertype=abstract.

[20] A. P. Ivanov, E. Instuli, C. M. McGilvery, G. Baldwin, D. W. McComb, T. Albrecht, and J. B. Edel, Nano Letters **11**, 279 (2011), ISSN 1530-6992, URL http://www.pubmedcentral.nih.gov/articlerender.fcgi?artid=3020087\&tool=pmcentrez\&rendertype=abstract.

[21] M. Zwolak and M. Di Ventra, Rev. Mod. Phys. **80**, 141 (2008), ISSN 0034-6861, URL http://link.aps.org/doi/10.1103/RevModPhys.80.141.

[22] H. He, R. H. Scheicher, R. Pandey, A. R. Rocha, S. Sanvito, A. Grigoriev, R. Ahuja, and S. P. Karna, Journal of Physical Chemistry C **112**, 3456 (2008), ISSN 1932-7447.

[23] K. S. Novoselov, A. K. Gueim, S. V. Morozov, D. Jiang, Y. Zhang, S. V. Dubonos, I. V. Grigorieva, and A. A. Firsov, Science **306**, 666 (2004).

[24] A. K. Geim and K. S. Novoselov, Nature Materials **6**, 183 (2007).

[25] A. H. Castro-Neto, F. Guinea, N. M. R. Peres, K. S. Novoselov, and A. K. Geim, Reviews of Modern Physics (2009).

[26] H. W. C. Postma, Nano Letters **10**, 420 (2010), ISSN 1530-6992, URL http://dx.doi.org/10.1021/nl9029237.

[27] C. A. Merchant, K. Healy, M. Wanunu, V. Ray, N. Peterman, J. Bartel, M. D. Fischbein, K. Venta, Z. Luo, A. T. C. Johnson, et al., Nano Letters **10**, 2915 (2010), ISSN 1530-6992, URL http://www.ncbi.nlm.nih.gov/pubmed/20698604.

[28] G. F. Schneider, S. W. Kowalczyk, V. E. Calado, G. Pandraud, H. W. Zandbergen, L. M. K. Vandersypen, and C. Dekker, Nano Letters **10**, 3163 (2010), ISSN 1530-6992, URL http://www.ncbi.nlm.nih.gov/pubmed/20608744.

[29] S. Garaj, W. Hubbard, A. Reina, J. Kong, D. Branton, and J. A. Golovchenko, Nature **467**, 190 (2010), ISSN 0028-0836, URL http://dx.doi.org/10.1038/nature09379.

[30] F. Traversi, C. Raillon, S. M. Benameur, K. Liu, S. Khlybov, M. Tosun, D. Krasnozhon, A. Kis, and A. Radenovic, Nature Nanotechnology **8**, 939 (2013), ISSN 1748-3387, URL http://www.nature.com/doifinder/10.1038/nnano.2013.240.

[31] T. Nelson, B. Zhang, and O. V. Prezhdo, Nano Letters **10**, 3237 (2010), ISSN 1530-6992, URL http://www.ncbi.nlm.nih.gov/pubmed/20722409.

[32] Y. He, R. H. Scheicher, A. Grigoriev, R. Ahuja, S. Long, Z. Huo, and M. Liu, Advanced Functional Materials **21**, 2674 (2011), ISSN 1616301X, URL http://doi.wiley.com/10.1002/adfm.201002530.

[33] J. Prasongkit, A. Grigoriev, B. Pathak, R. Ahuja, and R. H. Scheicher, Nano Letters **11**, 1941 (2011), ISSN 1530-6992, URL http://www.ncbi.nlm.nih.gov/pubmed/21495701.

[34] K. K. Saha, M. Drndić, and B. K. Nikolić, Nano Letters **12**, 50 (2012), ISSN 1530-6992, URL http://www.ncbi.nlm.nih.gov/pubmed/22141739.

[35] S. M. Avdoshenko, D. Nozaki, C. Gomes da Rocha, J. W. González, M. H. Lee, R. Gutierrez, and G. Cuniberti, Nano Letters **13**, 1969 (2013), ISSN 1530-6992, URL http://www.ncbi.nlm.nih.gov/pubmed/23586585.

[36] R. H. Scheicher, A. Grigoriev, and R. Ahuja, Journal of Materials Science (2012), ISSN 0022-2461, URL http://www.springerlink.com/index/10.1007/s10853-012-6671-0.

[37] J. Lagerqvist, M. Zwolak, and M. Di Ventra, Biophysical Journal **93**, 2384 (2007), URL http://arxiv.org/abs/0708.4395.

[38] A. Warshel and M. Levitt, Journal of Molecular Biology **103**, 227 (1976), ISSN 00222836, URL http://linkinghub.elsevier.com/retrieve/pii/0022283676903119.

[39] C. F. Sanz-Navarro, R. Grima, A. García, E. A. Bea, A. Soba, J. M. Cela, and P. Ordejón, Theoretical Chemistry Accounts **128**, 825 (2010), ISSN 1432-881X, URL http://link.springer.com/10.1007/s00214-010-0816-5.

[40] V. Hornak, R. Abel, A. Okur, B. Strockbine, A. Roitberg, and C. Simmerling, Proteins: Structure, Function, and Bioinformatics **65**, 712 (2006), ISSN 1097-0134, URL http://dx.doi.org/10.1002/prot.21123.

[41] H. Berendsen, D. van der Spoel, and R. van Drunen, Computer Physics Communications **91**, 43 (1995), ISSN 00104655, URL http://linkinghub.elsevier.com/retrieve/pii/001046559500042E.

[42] H. Berendsen, J. Postma, W. Gunsteren, and J. Hermans, in *Intermolecular Forces*, edited by B. Pullman (Springer Netherlands, 1981), vol. 14 of *The Jerusalem Symposia on Quantum Chemistry and Biochemistry*, pp. 331–342, ISBN 978-90-481-8368-5, URL http://dx.doi.

org/10.1007/978-94-015-7658-1_21.
[43] P. Hohenberg and W. Kohn, Physical Review **155**, B864 (1964), URL http://prola.aps.org/abstract/PR/v136/i3B/pB864_1.
[44] W. Kohn and L. J. Sham, Phys. Rev. **140**, A1133 (1965).
[45] J. P. Perdew, K. Burke, and M. Ernzerhof, Phys. Rev. Lett. **77**, 3865 (1996), URL http://link.aps.org/doi/10.1103/PhysRevLett.77.3865.
[46] J. M. Soler, E. Artacho, J. D. Gale, A. García, J. Junquera, P. Ordejón, and D. Sánchez-Portal, J. Phys. Cond. Mat. **14**, 2745 (2002).
[47] S. Datta, *Electronic Transport in Mesoscopic Systems* (Cambridge University Press, Cambridge, 1995), 1st ed.
[48] A. R. Rocha, V. M. Garcia-Suarez, S. W. Bailey, C. J. Lambert, J. Ferrer, and S. Sanvito, Nature Materials **4**, 335 (2005), ISSN 1476-1122.
[49] A. R. Rocha, V. García-Suárez, S. Bailey, C. Lambert, J. Ferrer, and S. Sanvito, Physical Review B **73** (2006), ISSN 1098-0121, URL http://link.aps.org/doi/10.1103/PhysRevB.73.085414.
[50] K. Nakada, M. Fujita, G. Dresselhaus, and M. S. Dresselhaus, Phys. Rev. B **54**, 17954 (1996), URL http://link.aps.org/doi/10.1103/PhysRevB.54.17954.